High-momentum particle production at hadron colliders

D M Adamiak[1,2],W A Horowitz[1]

[1]Department of Physics, University of Cape Town, Private Bag X3, Rondebosch 7701, South Africa

E-mail: [2] daniel.m.adamiak@gmail.com

Abstract. We compute the distributions of charged particles at large transverse momenta in pp, $p\bar{p}$, and pA collisions at Fermilab. Our calculations are performed using leading order perturbative quantum chromodynamics (pQCD), with both the usual parton distribution functions (PDFs) and nuclear PDFs, which encapsulate the modifications of the usual PDFs by the presence of multiple nucleons in a nucleus. We find that our results consistently describe the data at Fermilab, across multiple orders of magnitude in centre of mass energy $\sqrt{s}$, and over many orders of magnitude in transverse momentum. We then examine the transverse momentum dependence of the partonic contributions to these cross sections, which provides the critical input spectra for theoretical predictions for the suppression of charged particle spectra in heavy ion collisions.

1. Introduction

One of the current bleeding edges of physics concerns the question what arises from the emergent, many-body physics of quantum chromodynamics (QCD) at high-energies[1], such as that of the quark-gluon plasma. Analytically, one of the tools we use to make predictions for these phenomena is perturbative QCD (pQCD)[2]. Experimentally, one of the only available measurable quantities is the cross-section[3], in this a case a measurement of the spectrum of hadrons produced from an experiment. At colliders, such as those located at Fermi Lab[4] and CERN[5], we are able to to measure the charged hadron production of high energy collisions between protons, anti-protons and heavy nuclei. It is our area of interest to investigate how the partons, the constituent particles of the protons, behave in these collisions.

In high energy collisions it is impossible to directly observe the processes that the constituent partons undergo during the collision itself [6]. We are, however, able to control the input into the collision (particles used in the collision and their energies) as well as measure the output (hadron production and energy spectrum). Using pQCD we make predictions about how the partons behave during these collisions, with this behaviour producing its own prediction spectrum that we are able to compare with the data.

We use the result derived by Eskola and Honkanen [7] using Leading Order pQCD to calculate the differential cross-section of charged hadron production in pp collisions. The calculation is performed numerically, with the results being compared to Eskola and Honkanen' computation. Since they have already demonstrated that the theory agrees strongly with data, we compare only with their calculation to confirm whether we have performed our computation correctly. Agreement with their calculation within machine precision implies agreement with data.

After finding strong agreement with the experimental data, we break down the cross-section into the contributions due to each parton and their dependence on transverse momentum. The long-term goal is to use these results as an input for theoretical predictions for the suppression of charged particle spectra in heavy ion collisions [8].

Both calculations can also be done for the pA collision case, a collision between a proton and either a lead or a gold nucleus. This calculation for pp collisions is modified by introducing a nuclear PDF (nPDF) into our calculations.

2. Leading Order pQCD Calculations

We calculate the inclusive cross-section for production of a parton of a flavour f and a rapidity y_f in Mathematica. The expression for this cross-section, derived using pQCD, is given by [7]

$$\begin{aligned}\frac{d\sigma^{AB\to h+X}}{dq_T^2 dy_f} &= K(\sqrt{s})J(m_T,y)\int\frac{dz}{z^2}\int dy_2 \sum_{<ij><kl>}\frac{1}{1+\delta_{kl}}\frac{1}{1+\delta_{ij}}\times \\ &\times\Bigg\{x_1 f_{i/A}(x_1,Q^2)x_2 f_{j/B}(x_2,Q^2)\left[\frac{d\hat{\sigma}}{d\hat{t}}^{ij\to kl}(\hat{t},\hat{u})\underset{k\to h}{D}(z,\mu_F^2)+\frac{\hat{\sigma}}{d\hat{t}}^{ij\to kl}(\hat{u},\hat{t})\underset{l\to h}{D}(z,\mu_F^2)\right] \\ &+\quad x_1 f_{j/A}(x_1,Q^2)x_2 f_{i/B}(x_2,Q^2)\left[\frac{d\hat{\sigma}}{d\hat{t}}^{ij\to kl}(\hat{u},\hat{t})\underset{k\to h}{D}(z,\mu_F^2)+\frac{\hat{\sigma}}{d\hat{t}}^{ij\to kl}(\hat{t},\hat{u})\underset{l\to h}{D}(z,\mu_F^2)\right]\Bigg\}\end{aligned} \tag{1}$$

where y_2 and y_f are the rapidities of the outgoing partons. $x_1 = \frac{p_T}{\sqrt{s}}(e^{y_f}+e^{y_2})$, $x_2 = \frac{p_T}{\sqrt{s}}(e^{-y_f}+e^{-y_2})$. z is a parameter equal to the ratio of the energy of the quark, f, to hadron h. $\sqrt{s}$ is the root center of mass energy, the energy in the rest frame of the interaction. Present are the differential cross-sections of parton interactions, $\frac{d\hat{\sigma}}{d\hat{t}}$ and the Mandelstam variables, $\hat{t},\hat{u}$. Also present are the PDFs, f and fragmentation functions, D. J is a function defined by

$$J(m_T,y) = (1-\frac{m^2}{m_T^2\cosh^2 y})^{-1/2} \tag{2}$$

where m is the mass of the outgoing hadron and m_T is the transverse mass of the outgoing hadron. The sum over i,j,k,l is a sum over every possible interaction, where i,j,k,l stand for labels of the the different partons(quarks, anti-quarks and gluons). The constant, K, is the ratio of the experimental cross-section to the leading order cross-section. It was found by Eskola and Honkanen in their paper [7] that K was a function only of $\sqrt{s}$ and encapsulates the next-to-leading order contributions.

What is being described by this integral, roughly, is that the probability of h being formed at momentum q_T, is equal to the sum over every possible interaction that could form h with momentum q_T.

2.1. Parton Distribution Functions

When a proton is moving with some momentum, each of it's constituent partons carries a fraction of that momentum. These constituent partons include the uud quarks, the gluons binding them and all the virtual quarks inside the proton as well. This way it is possible for, say, the strange quarks to carry some momentum fraction of the proton as well. The ratio of momentum each constituent parton carries to the total momentum is known as the Parton Distribution Function (PDF)[9]

These are not analytic functions, but rather a polynomial interpolation of recorded PDF values. Originally written in FORTRAN, the code was adapted to Mathematica by us, available

on request. The PDF is a function f that takes two input parameters, fractional momentum x and energy scale Q. While, in general, the PDF does not have to be of a proton, that is what we are considering here. In our calculation, the parton distribution function of [10] is used.

For pA collisions, we modify the PDF by a nuclear parton distribution function (nPDF). It is another polynomial interpolation originally written by in FORTRAN [11], adapted to Mathematica by us. The way the nPDFs were constructed is that, given an input energy, transverse momentum and nucleus size, they produce a modification factor which we multiply into the PDF of the parton that we choose to come from the heavier nucleus. This will give us the differential cross-section of a pA collision.

2.2. Fragmentation Functions

Fragmentation functions, D, describe transition of a parton, f, with some fractional momentum, z, at some energy scale, μ_F, into a hadron, h.[12]. Again, we have no analytic function at hand. We use the fragmentation functions found in [13]. We use the same functions adapted for Mathematica

3. Modification to extract partonic contributions

We now modify our calculation so that we can calculate the individual contribution to the total cross-section from each parton. The modification is quite simple. Examining equation(1), we eliminate the fragmentation functions, since these are used to tell us about the formation of hadrons. This leaves us with a calculation about the production of partons.

The second modification is that, rather than summing over all the partons, we record the contribution due to each parton separately. Our calculation then looks like

$$\begin{aligned}\frac{d\sigma^{AB\to k+X}}{dq_T^2 dy_f} = \int dy_2 \sum_{<ij><kl>} \frac{1}{1+\delta_{kl}} \frac{1}{1+\delta_{ij}} \times \\ \times x_1 f_{i/A}(x_1, Q^2) x_2 f_{j/B}(x_2, Q^2) \left[\frac{d\hat{\sigma}^{ij\to kl}}{d\hat{t}}(\hat{t}, \hat{u})\right]\end{aligned} \tag{3}$$

where, once again, i, j, k, l represent each of the participating partons where we now save the result for the k outgoing partons individually.

4. Results

In figure 1, we compare our calculated differential cross-section with the calculation from figure 5 of [7], which was, in turn, used to make a prediction for [14]

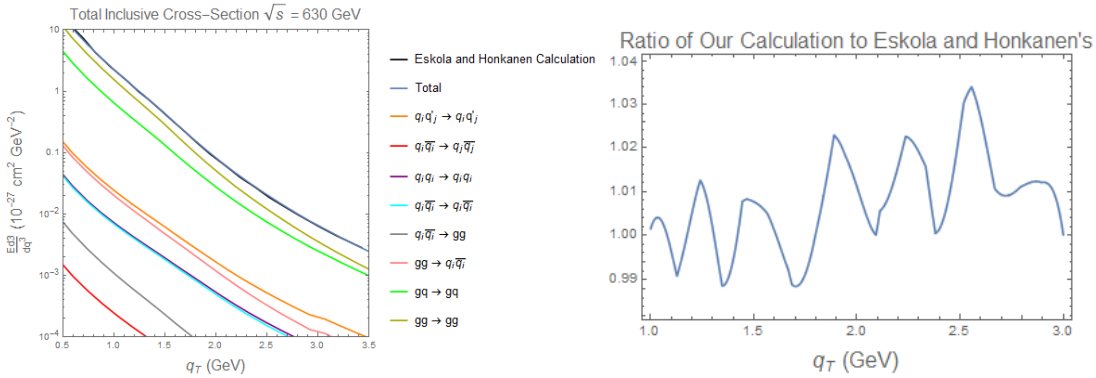

Figure 1: (Left) Calculated differential cross-section of $p\bar{p}$ production at $\sqrt{s} = 630$ GeV(blue), compared with the calculation from Eskola and Honkanen (black), as well as the contributions to the total cross-section from each of the possible partonic interactions. (Right) The ratio of our calculation to the calculation from Eskola and Honkanen.

The first plot of figure 1 is a plot of our calculated differential cross-section of charged hadron production of $p\bar{p}$ collisions at $\sqrt{s} = 630$ GeV as a function of q_T compared with the calculation performed in [7]. Also included are the contributions from the various processes that make up the total cross-section when summed over. The plot on the left of figure 1 is a plot of the ratio of our calculated cross-section to the calculation in 1. Agreement within four percent implies that we have implemented our calculation correctly. The four percent discrepancy is attributed to machine precision error and is small compared to other sources of uncertainty, for example in figure 5 of [7], their K value has an uncertainty of 18%

Next we give a result of our parton contribution calculation. We perform the calculation at many energies to match the energies used in experiment, but, in figure 2, we just show the result for $\sqrt{s} = 200$ GeV.

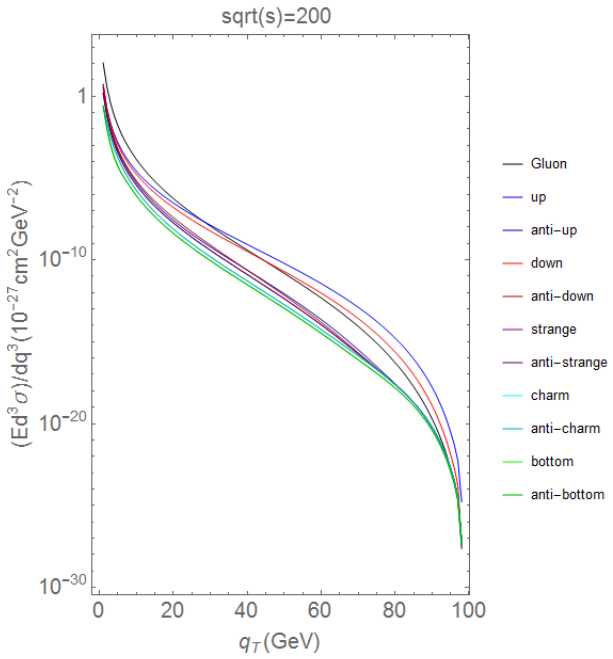

Figure 2: Parton conrtibutions to the total differential cross-section

We find that at low energies, the gluons are the leading source to the cross-section. At higher energies we find that the valence quarks dominate the spectrum. This is inferred from the spectrum containing a leading contribution from the up and down quarks in a 2-1 ratio, the make-up of a proton.

5. Conclusion

Using the methods of pQCD, we have made a prediction for the behaviour of partons within a $p\bar{p}$ collision. These partonic contributions were used as an input to compute the total differential cross-section. When compared with the calculation in [7], strong agreement was found. This implies that our calculation agrees with the data strongly. From this we conclude that either our partonic contributions were calculated correctly, or that any unaccounted for effects perfectly cancelled each other out when we computed the cross section. Assuming the former, we can use this partonic contributions as a critical input for energy loss calculations.

The next step would be to modify the calculations for pA collisions to see if they match the measured data and predicted results. The partonic contributions from a pA, when used as an input for energy loss calculations, can be used to explore the effect of the medium, if any, present in pA, but not in $p\bar{p}$ collisions.

References

[1] The Frontiers of Nuclear Science, A Long Range Plan. 2008.

[2] K. Kajantie and Hannu Kurki-Suonio. Bubble growth and droplet decay in the quark-hadron phase transition in the early universe. *Phys. Rev. D*, 34:1719–1738, Sep 1986.

[3] L.P. Remsberg T. Abbott, L. Kowalski. Rapidity and invariant cross sections.

[4] James Green. A Measurement of High Transverse Momentum Charged Hadron Production Using a Pion Beam and Hydrogen Target. 1981.

[5] The ATLAS collaboration. Charged hadron production in p+Pb collisions at $\sqrt{s_{\rm NN}} = 5.02$ TeV measured at high transverse momentum by the ATLAS experiment. 2014.

[6] B. Povh, M. Lavelle, and M. Rosina. *Scattering and Structures: Essentials and Analogies in Quantum Physics*. Number p. 66713 in Scattering and Structures: Essentials and Analogies in Quantum Physics. Springer Berlin Heidelberg, 2005.

[7] K. J. Eskola and H. Honkanen. A Perturbative QCD analysis of charged particle distributions in hadronic and nuclear collisions. *Nucl. Phys.*, A713:167–187, 2003.

[8] K. Aamodt et al. Suppression of Charged Particle Production at Large Transverse Momentum in Central Pb-Pb Collisions at $\sqrt{s_{NN}} = 2.76$ TeV. *Phys. Lett.*, B696:30–39, 2011.

[9] M Dittmar, S Forte, A Glazov, S Moch, S Alekhin, Guido Altarelli, J Andersen, R D Ball, J Blmlein, Helmut B Bttcher, T Carli, Marcello Ciafaloni, D Colferai, A Cooper-Sarkar, Gennaro Corcella, L Del Debbio, G Dissertori, J Feltesse, A Guffanti, C Gwenlan, J Huston, G Ingelman, M Klein, J I Latorre, T Lastoviicka, G Lastoviicka-Medin, L Magnea, A Piccione, J Pumplin, V Ravindran, B Reisert, J Rojo, Agustin Sabio Vera, Gavin P Salam, F Siegert, A M Stasto, H Stenzel, C Targett-Adams, R S Thorne, A Tricoli, J A M Vermaseren, and A Vogt. Introduction to parton distribution functions. 2005.

[10] H. L. Lai, J. Huston, S. Kuhlmann, J. Morfin, Fredrick I. Olness, J. F. Owens, J. Pumplin, and W. K. Tung. Global QCD analysis of parton structure of the nucleon: CTEQ5 parton distributions. *Eur. Phys. J.*, C12:375–392, 2000.

[11] K. J. Eskola, H. Paukkunen, and C. A. Salgado. EPS09: A New Generation of NLO and LO Nuclear Parton Distribution Functions. *JHEP*, 04:065, 2009.

[12] D de Florian and D Milstead. 17. fragmentation functions in e e-, ep and pp collisions.

[13] Bernd A. Kniehl, G. Kramer, and B. Potter. Fragmentation functions for pions, kaons, and protons at next-to-leading order. *Nucl. Phys.*, B582:514–536, 2000.

[14] F. Abe et al. [CDF Collaboration]. *Phys. Rev. Lett. 61 1819*, 1988.